Zeeman and Davydov splitting of Frenkel excitons in the antiferromagnet CuB_2O_4

N. E. Kopteva,[1] D. Kudlacik,[1] D. R. Yakovlev,[1,2] M. V. Eremin,[3] A. R. Nurmukhametov,[3] M. Bayer,[1,2] and R. V. Pisarev[2]

[1]*Experimentelle Physik 2, Technische Universität Dortmund, 44221 Dortmund, Germany*
[2]*Ioffe Institute, Russian Academy of Sciences, 194021 St. Petersburg, Russia*
[3]*Institute of Physics, Kazan Federal University, 420008 Kazan, Russia*

(Received 3 November 2021; accepted 13 January 2022; published 27 January 2022)

The optical spectra of antiferromagnetic copper metaborate CuB_2O_4 are characterized by an exceptionally rich structure of narrow absorption lines due to electronic transitions within the magnetic Cu^{2+} ions, but their unambiguous identification and behavior in magnetic fields have remained far from being fully understood. We study the polarized magnetoabsorption spectra of this tetragonal antiferromagnet with high spectral resolution across the energy range of 1.4055–1.4065 eV in magnetic fields up to 9.5 T for temperatures from 1.6 up to the Néel temperature $T_N = 20$ K. We observe a set of eight absorption lines at $T = 1.6$ K in magnetic fields exceeding 1.4 T, which we identify as arising from Frenkel excitons related to the ground and first excited states of the Cu^{2+} ions. The number of these excitons is defined by the presence of the four Cu^{2+} ions with doubly degenerate spin state $S = 1/2$ at the 4*b* positions in the crystallographic unit cell. The energies of these excitons are determined by the exchange interaction of 0.5 meV of the Cu^{2+} ions in the excited state with the surrounding ions and by the Davydov splitting of 0.12 meV. In large magnetic field the observed Zeeman splitting is controlled by the anisotropic *g*-factors of both the ground and excited states. We develop a theoretical model of Frenkel excitons in the magnetic field that accounts for specific features of the spin structure and exchange interactions in CuB_2O_4. The model is used for fitting the experimental data and evaluation of the Frenkel exciton parameters, such as the Davydov splitting, the molecular exchange energy, and the *g*-factors of the ground and excited states of the Cu^{2+} ions.

DOI: 10.1103/PhysRevB.105.024421

I. INTRODUCTION

The compound with the chemical formula CuB_2O_4 has been known for over a hundred years [1], but its crystal structure was resolved only in 1971 [2] and later refined in 1981 [3]. This material has received a lot of attention during the last two decades due to its intriguing magnetic, optical, magnetooptical, and nonlinear optical properties. The magnetic phase diagram of CuB_2O_4 below $T_N = 20$ K [4] is very complicated and includes commensurate and incommensurate phases and also phases of unknown structure. The phase transitions of different types are sensitive to temperature and applied magnetic field [4–6].

The optical absorption spectra of CuB_2O_4 below T_N are characterized by an abundantly large number of very narrow lines, some of which were identified with purely electronic transitions of the Cu^{2+} ions, others with phonon sidebands [7,8]. Below T_N, both the spatial inversion and the time reversal symmetry are broken, which opens up new possibilities for observing unusual optical phenomena. Some examples are the magnetic-field-induced optical second harmonic generation [7,9], the giant optical magnetoelectric effect [10], the one-way transparency for light [11], and some others [12]. The very unusual effect of a direction-dependent luminescence induced by a magnetic field was observed in the photoluminescence of CuB_2O_4 [13]. Note that the efficient photoluminescence of CuB_2O_4 [13,14] by itself is quite surprising for Cu^{2+} oxide compounds. A huge resonant nonreciprocity reaching almost 100% under the reversal of an applied magnetic field was recently observed in studies of optical second harmonic generation in the range of the lowest-in-energy electronic transition around 1.4055–1.4061 eV [15,16]. Some observations related to the action of a magnetic field on the optical effects, in particular concerning optical chirality, raised an intense dispute between experimental and theoretical groups about possible explanations [17–20].

Despite the significant number of experimental studies of different optical effects in CuB_2O_4, until now their explanation has mostly remained at the macroscopic level, where only the factors determining the crystallographic and magnetic symmetries at temperatures below T_N are taken into account [21]. However, the origin and understanding of the observed effects at the microscopic level are still unclear since the details of the electronic structure of the excited states of the magnetic Cu^{2+} ions have remained unexplored. It was suggested that some of them can be related to the Davydov splitting of excited states [22] because CuB_2O_4 is an antiferromagnet in which the magnetic Cu^{2+} ions occupy two types of crystallographically nonequivalent positions in the unit cell [2]. Namely, there are four of these ions in the 4*b* magnetic subsystem and eight ions in the 8*d* subsystem. Thus, the narrow absorption lines observed in previous experiments

serve as a solid input for testing the Frenkel exciton concept and developing a detailed microscopic model.

In the papers of Frenkel [23,24] and Davydov [25,26], the Coulomb interaction, or more precisely its expansion in multipole moments, was suggested to be responsible for resonant excitation transfer between the equivalent ions in a crystallographic unit cell or in a single molecule. The concept of Frenkel excitons in the optical spectra of insulating antiferromagnets was first suggested in a review paper by Loudon [27], but it could only be applied to a few materials for which the absorption lines are sufficiently narrow to allow studying the magnetic field effects on the exciton states.

The most exemplary materials in that respect are the Cr^{3+}-based antiferromagnets, such as Cr_2O_3 [28] and the rare-earth (R) orthochromites $RCrO_3$ [29,30]. Their optical absorption spectra show narrow lines with widths of hundred μeV, which is unusual for most of the antiferromagnetic oxides. Davydov splittings comparable with the linewidth were reported. However, later the interpretation of the Davydov splittings given in these papers was criticized in Ref. [31], where the Davydov splitting of excitons in Cr_2O_3 was studied experimentally and theoretically in great detail. It was shown that the previous interpretations conflict with the results of a group-theory analysis concerning the interionic exchange interactions and the effect of an applied magnetic field, and a new assignment of the exciton lines was suggested. Soon after the detailed theoretical analysis was extended to the excitons in $YCrO_3$, which showed that previous conclusions on the exciton level structure should be reconsidered [32–34].

The problem is that the magnetic field effects, which prove the involvement of the spin degrees of freedom in the formation of band excitations, were observed only on the four lines in the absorption spectra of Cr^{3+}-based antiferromagnets. However, taking into account the general idea about the number of Davydov-split Frenkel exciton states, the number of lines should be larger. Indeed, there are four Cr^{3+} ions in the unit cell of Cr_2O_3 and $RCrO_3$ crystals. In this case, each of the excited ^{2}E states of the Cr^{3+} ions is twofold degenerate in the orbital and twice in the spin ($S_z = \pm 1/2$) variables. Thus, 16 exciton states at $k = 0$ are expected to be present, but only four lines were resolved in the absorption spectra of Cr_2O_3 and $RCrO_3$ crystals. We are not aware of any publication of experimental results on the observation of the entire set of Davydov-split Frenkel exciton states.

The goal of our present paper is to study experimentally and explain theoretically on a microscopic level the fine structure of the Davydov-split Frenkel excitons in CuB_2O_4 in the 1.4055–1.4065 eV spectral range of the electronic transitions in the 4b subsystem of the Cu^{2+} ions. Similar to the Cr^{3+}-based antiferromagnets discussed above, the unit cell of CuB_2O_4 contains four magnetic Cu^{2+} ions at the 4b positions. However, in contrast to chromium compounds, in which the spin $S = 3/2$ in the ground state, and $S = 1/2$ in the excited state, in CuB_2O_4 the spin $S = 1/2$ in both the ground $|\epsilon\rangle = |x^2 - y^2\rangle$ and excited $|\zeta\rangle = |xy\rangle$ states. Thus, both the ground and excited states of the Cu^{2+} 4b ions are orbitally nondegenerate and the maximum number of exciton states should be eight when the two spin ($S_z = \pm 1/2$) states are taken into account. We succeeded in measuring these eight exciton states in absorption and trace their behavior in external magnetic fields up to 9.5 T for the temperature range of 1.6–20 K. To the best of our knowledge, this is the first observation of the full set of the Davydov-split Frenkel exciton states in antiferromagnets. We developed a microscopic theory, which explains well the experimental observation of Davydov-split Frenkel excitons in CuB_2O_4.

The paper is organized as follows. In Sec. II, we discuss the crystal structure and the magnetic and optical properties of CuB_2O_4 on the basis of previous studies. In Sec. III, the experimental details are given. In Sec. IV, we present the experimental results on the absorption spectra of the lowest-energy electronic transition in strong magnetic fields at cryogenic temperatures. In Sec. V, a detailed theoretical analysis of the Davydov-split Frenkel exciton states is presented. Section VI is devoted to the modeling of the experimental results on the basis of the developed theory of the properties of the Davydov-split Frenkel exciton states in a magnetic field applied along one of the main crystallographic axes. In Sec. VII, we summarize in brief the experimental and theoretical results.

II. CRYSTAL STRUCTURE, MAGNETIC, AND OPTICAL PROPERTIES OF CuB_2O_4

The crystallographic unit cell of CuB_2O_4 contains 12 formula units and the crystal structure is described by the tetragonal noncentrosymetric point group $\bar{4}2m$ (D_{2d}) and the space group $I\bar{4}2d$ (D_{2d}^{12}) [2,3]. The unit cell contains 12 magnetic copper ions Cu^{2+} ($3d^9$ electronic shell, $S = 1/2$), which occupy the 4b and 8d crystallographically different positions with the site symmetry $\bar{4}$ and 2, respectively. Above the Néel temperature of $T_N = 20$ K [4], CuB_2O_4 is in the paramagnetic phase and both the 4b and 8d magnetic subsystems of the Cu^{2+} ions are disordered. Below T_N, the 4b subsystem is antiferromagnetically ordered, while the 8d subsystem is in a partially ordered state down to the lowest temperatures [5]. We restrict our experimental studies and theoretical analysis to the optical absorption in the spectral range of 1.4055–1.4061 eV that is related to the lowest exciton transitions in the 4b magnetic Cu^{2+} subsystem.

Figure 1(a) shows the spin structure of the 4b Cu^{2+} subsystem in the commensurate antiferromagnetic phase where the spins are oriented along the [110] axis in zero magnetic field. In the basis of the four 4b spins $\mathbf{S}_i$ ($i = \alpha, \beta, \gamma$, and δ) in the unit cell, the two ferromagnetic $\mathbf{M}$ and antiferomagnetic $\mathbf{L}$ order parameters in the commensurate phase can be written as $\mathbf{M} = \mathbf{S}_\alpha + \mathbf{S}_\beta + \mathbf{S}_\gamma + \mathbf{S}_\delta$ and $\mathbf{L} = \mathbf{S}_\alpha - \mathbf{S}_\beta + \mathbf{S}_\gamma - \mathbf{S}_\delta$ [5]. Figure 1(a) shows the Cu^{2+} ions located in different ab layers along the c axis in which the spins are marked in light blue (α), blue (β), red (γ), and brown (δ) color. The arrows give the Cu^{2+} spin directions along the [110] axis in the ground antiferromagnetic state without external magnetic field.

Previous studies showed that the optical absorption of CuB_2O_4 in the near-infrared and visible spectral range from 1.4 up to 2.5 eV arises from electronic transitions within the $3d^9$ electronic states of the Cu^{2+} ions, which are split by the crystal field at the two crystallographic positions [7,8]. These transitions provide exceptionally rich and highly polarized spectra with absorption coefficients reaching values above 600 cm^{-1}. The transparency window between 2.5 and

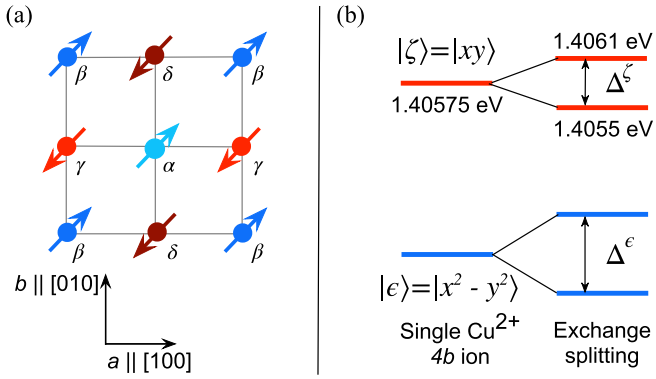

FIG. 1. (a) Projection along the tetragonal c axis of the antiferromagnetic structure of CuB_2O_4 for the $4b$ magnetic subsystem in the commensurate phase at zero magnetic field. Here the c axis points along the [001] crystal direction and the ab basal plane is spanned by the $a \parallel [100]$ and $b \parallel [010]$ crystal directions. Only a single antiferromagnetic domain is shown in which the spins S_i are oriented along the [110] axis, whereas in other domains the spins may be oriented along the $[\bar{1}10]$, $[\bar{1}\bar{1}0]$, and $[1\bar{1}0]$ axes. (b) Energy level diagram of the ground $|\epsilon\rangle = |x^2 - y^2\rangle$ and the first excited $|\zeta\rangle = |xy\rangle$ states of a single $4b$ Cu^{2+} ion, which are split by the exchange interaction $\Delta^{\epsilon(\zeta)}$ with neighboring Cu^{2+} ions from the $4b$ and $8d$ (not shown) subsystems. The splittings Δ^ϵ and Δ^ζ are different in the ground and excited states, as will be shown below in Sec. V.

3.5 eV causes the blue color of CuB_2O_4 single crystals [8]. According to recent ellipsometric studies, strong absorption with coefficients reaching 10^6 cm^{-1} due to parity-allowed charge-transfer transitions sets in at about 4.0 eV [35].

In this paper we focus solely on the electronic transition of the Cu^{2+} ions with lowest photon energy in the range of 1.4055–1.4061 eV. The underlying energy level diagram of the ground and excited states is schematically shown in Fig. 1(b). The electronic transitions take place between the orbitally nondegenerate ground $|\epsilon\rangle = |x^2 - y^2\rangle$ and excited $|\zeta\rangle = |xy\rangle$ states of a single Cu^{2+} ion [7,8,22]. Due to the exchange interaction of the Cu^{2+} ion with its surrounding ions in the $4b$ and $8d$ subsystems, these states are split by the energies Δ^ζ and Δ^ϵ, respectively. The main goal of our paper is to show that this single-ion scheme used in several previous publications describing optical experiments in this spectral region should be seriously revised due to the presence of the four $4b$ Cu^{2+} ions in the elementary crystal unit cell [2] interacting with the surrounding Cu^{2+} ions from both the $4b$ and $8d$ magnetic subsystems. The concept of Frenkel excitons with a Davydov splitting is applied for explaining the experimentally observed fine-structure of the absorption in an applied magnetic field.

III. EXPERIMENTAL DETAILS

Single crystals of CuB_2O_4 were grown by the Kyropoulos technique from a melt of B_2O_3, CuO, Li_2O, and MoO_3 oxides [7–9,36]. To ensure a well-defined orientation of the samples, plane-parallel polished plates were cut from single crystals oriented using Laue x-ray diffraction.

Two samples were studied, namely a (001) sample with the optical c-axis oriented along the sample normal [see Fig. 2(a)], $c \parallel [001]$, and a (101) sample with the optical axis $c \parallel [001]$ in the sample plane [see Fig. 2(b)]. The ab basal plane in the (001) sample is perpendicular to the [001] crystal direction and is spanned by the two a and b crystallographic axes ($a \parallel [100]$ and $b \parallel [010]$).

The 1.12-mm thick (101) sample was used for reliable recording of π spectra with absorption on the order of 10 cm^{-1} for which the light wave vector $\mathbf{k} \parallel b$ and the polarization of the incident light $\mathbf{E} \parallel c$, where the nomination of the spectra is for indicating their polarization. The (001) sample with a thickness of 59 μm was used to detect the α spectra recorded in the geometry $\mathbf{k} \parallel c$ and $\mathbf{E} \parallel a$.

The samples were mounted strain-free in a split-coil magnet cryostat and measurements were performed in the temperature range 1.6–20 K. The magnetic field was oriented perpendicular to the $\mathbf{k}$ vector of light (Voigt geometry) and its strength was tuned from 0 up to 9.5 T. The (101) sample was rotated in the ac plane by 90° to obtain the geometry with $\mathbf{B} \parallel c$ and $\mathbf{B} \parallel a$, Figs. 2(c) and 2(d), respectively.

For investigating the absorption spectra in the spectral range from 1.35 to 2.5 eV, the white light emission of a halogen lamp was used. The power density of the light source was set to 5 $\mu W/mm^2$. The light was linearly polarized by a Glan-Thompson prism. A $\lambda/2$ retardation plate was used for rotating the linear polarization between the vertical and horizontal orientations. To avoid any influence of the polarization characteristics of the grating spectrometer, we coupled light of a fixed linear polarization into the entrance slit. For that, after transmission through the sample the light was analyzed by a $\lambda/4$ retardation plate with its optical axis oriented at 45° followed by a Glan-Thompson prism. The transmitted light was spectrally resolved by a 1 m Spex spectrometer equipped with a 10×10 cm^2 sized grating having 1200 grooves/mm used in first order. A silicon charge-coupled device (CCD) camera with 512×2048 pixels of 13.5 μm size was used as detector. In combination with a 4× magnification optics in front of the CCD camera, it was possible to improve the spectral resolution to 20 μeV.

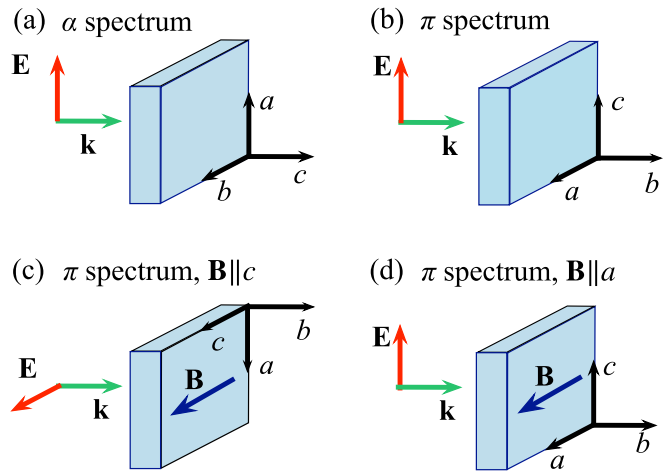

FIG. 2. Schemes of the orientation of the sample axes relative to the $\mathbf{k}$-vector of light and the light polarization vector $\mathbf{E}$ for the (a) α and (b) π spectra. The magnetic field is applied in the Voigt geometries (c) $\mathbf{k} \perp \mathbf{B} \parallel c$ and (d) $\mathbf{k} \perp \mathbf{B} \parallel a$ for measuring π spectra.

IV. EXPERIMENTAL RESULTS

A. Absorption spectra in zero magnetic field

The low-temperature absorption spectra of CuB_2O_4 in the energy range of 1.4–2.5 eV for three main polarizations (α, σ, and π) are characterized by a rich structure of zero-phonon (ZP) lines related to the Cu^{2+} ions in the $4b$ and $8d$ sublattices [7,8,22]. Each ZP line is accompanied by a long tail of phonon sidebands. Here we focus exclusively on the set of absorption lines originating from the first ZP line related to the $4b$ subsystem within the 1.4055–1.4061 eV spectral range. The α and π spectra measured in the (001) and (101) samples are shown in Figs. 3(a) and 3(b), respectively.

The observed asymmetric line originates from the optical transition between the ground $|\epsilon\rangle = |x^2 - y^2\rangle$ and the excited $|\zeta\rangle = |xy\rangle$ states of the Cu^{2+} ions [7,8,22]. The asymmetric shape suggests the presence of at least two partially overlapping lines with different amplitudes, the parameters of which we evaluate from the double Gaussian fits shown by the green and blue areas in Fig. 3. We refer to the lines at the lower 1.4055 eV and the higher 1.4061 eV photon energy as A and B lines, respectively. The intensity ratio between the lines is $I_B/I_A = 3.32$ and 3.25 for the σ and π spectra, respectively. The energy splitting between the A and B lines amounts to $\Delta^\zeta = 0.5$ meV. Both lines have similar full widths at half maximum (FWHMs) of $W_A = 0.44$ meV and $W_B = 0.56$ meV. These lines can be identified as originating from Frenkel excitons.

It is worth noting here that this zero-field splitting of the ZP absorption line, as well as the luminescence line, was previously already noted in Refs. [14,22], respectively. The observed ZP line splitting is puzzling because the relevant electronic transition takes place between the ground and excited states of a single Cu^{2+} ion which are both orbitally nondegenerate. A tentative assignment of the doublet structure to the Davydov splitting was suggested due to the presence of two copper Cu^{2+} ions in the primitive unit cell [22]. In our paper, on the basis of experiments at low temperatures in high magnetic field, supplemented by a microscopic theoretical analysis, we present a detailed microscopic model of the Davydov splitting of Frenkel excitons in CuB_2O_4.

It is important that both the ground and excited electronic states of the Cu^{2+} ions do not interact with the electric field of the light wave because they have the even parity of their $3d^9$ wave functions [38]. Therefore, transitions between them are forbidden in the electric-dipole (ED) approximation. However, the local crystal field acting on the Cu^{2+} ions leads to a mixing of the even $|\epsilon\rangle = |x^2 - y^2\rangle$ ground state with the odd $3d^8 4p^1$ and charge-transfer-excited configurations. Due to the odd crystal field components, the mixing between these configurations of opposite parity and the oxygen-copper electron transfer process activate the optical transitions both in the ED and MD approximations [39,40].

B. Magnetoabsorption spectra of Frenkel excitons at $T = 1.6$ K

The application of a magnetic field is a powerful tool in exciton spectroscopy that allows one to disclose the fine-structure of electronic levels and uniquely identify the exciton states using their Zeeman splittings and polarization features. In magnetically ordered materials, an applied magnetic field can induce phase transitions, which can also affect the exciton states.

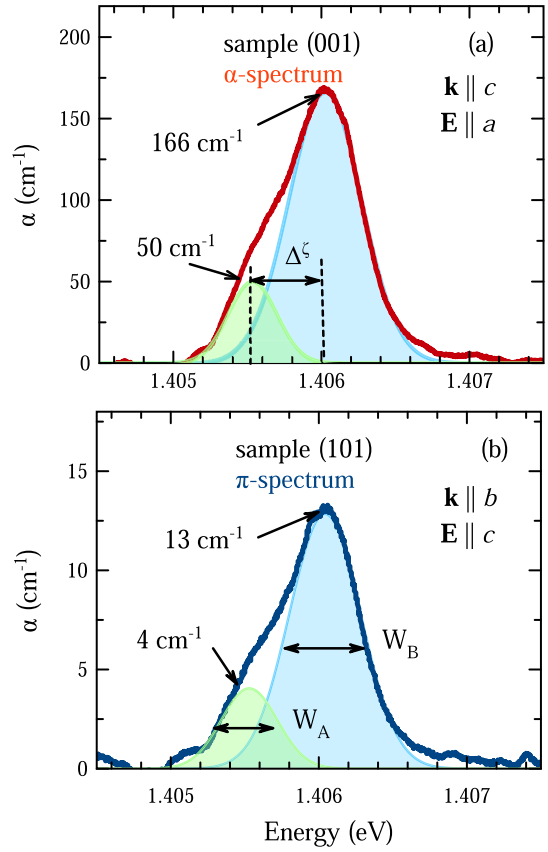

FIG. 3. Polarized absorption spectra of CuB_2O_4 in the spectral range of the lowest photon-energy transition from the ground $|\epsilon\rangle = |x^2 - y^2\rangle$ state to the lowest-in-energy excited $|\zeta\rangle = |xy\rangle$ state of the Cu^{2+} ions at the $4b$ positions [7,8,22]. The spectra were measured at $T = 1.6$ K in zero magnetic field for the two geometries corresponding to (a) the α-configuration when $\mathbf{k} \parallel c$ and $\mathbf{E} \parallel a$, measured on the (001) sample, and (b) the π-configuration when $\mathbf{k} \parallel b$ and $\mathbf{E} \parallel c$, measured on the (101) sample. The absorption coefficients in the two spectra differ by more than an order of magnitude. According to the selection rules for absorption in uniaxial crystals, the α and π spectra correspond to the electric-dipole (ED) and magnetic-dipole (MD) transitions, respectively [37]. The green- and blue-shaded areas represent Gaussian fits used for evaluation of the exciton parameters. The FWHMs are indicated by $W_{A(B)}$. The doublet splitting assigned to the excited state is denoted by Δ^ζ.

We study the modification of the exciton absorption spectra in π geometry (see Fig. 2) for magnetic fields up to 9.5 T at $T = 1.6$ K. The magnetoabsorption results for the (101) sample are collected in Fig. 4 for two magnetic field orientations along the main a and c crystallographic axes. The results are presented comprehensively by showing the absorption spectra, their contour maps, and the field dependencies of the line maxima.

Let us first consider the $\mathbf{B} \parallel c$ configuration, presented in the upper row of panels in Fig. 4. One can see in Fig. 4(a) that

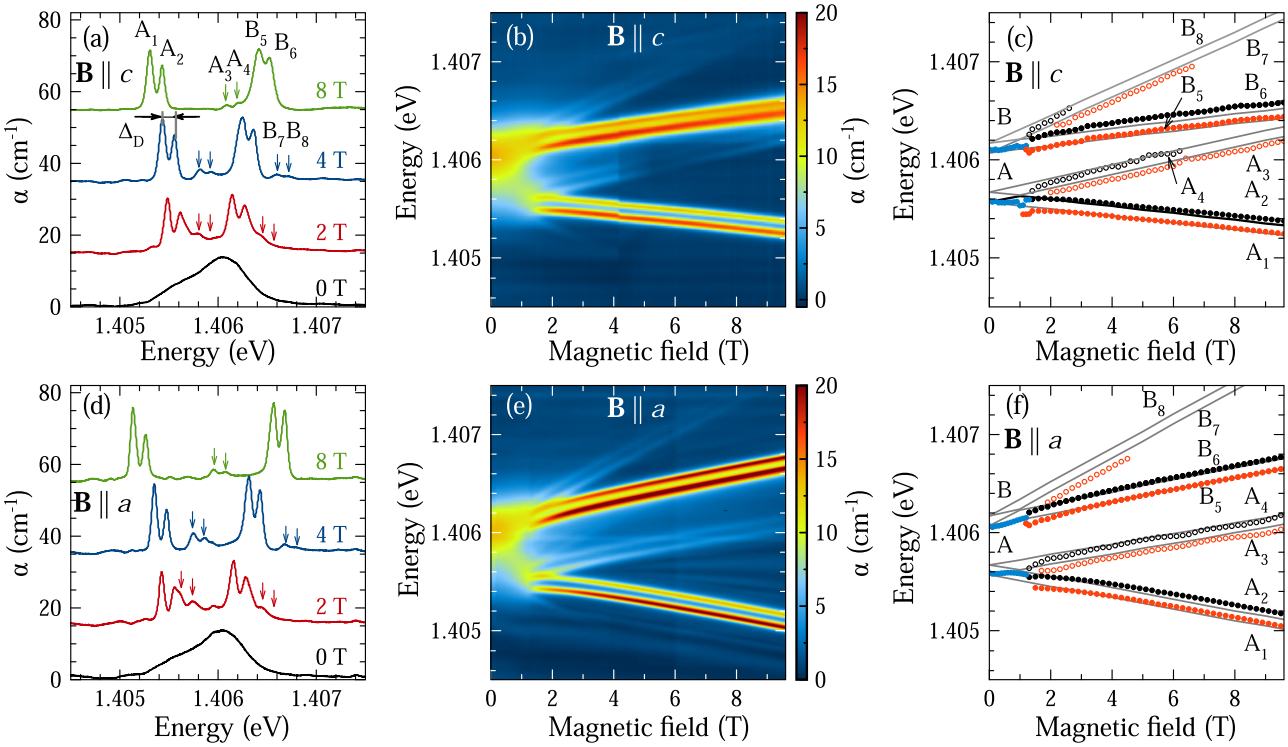

FIG. 4. Evolution of the absorption spectra showing the Frenkel excitons due to optical transitions between the ground and excited states of the Cu^{2+} ions within the 4*b* sublattice. The π spectra in all panels are measured at $T = 1.6$ K for the (101) sample. The results in panels (a), (b), and (c) are recorded in the $\mathbf{B} \parallel c$ configuration. The results in panels (d), (e), and (f) are recorded in the $\mathbf{B} \parallel a$ configuration. Panels (b) and (e) are contour plots where the absorption amplitude is encoded in the color. The magnetic field dependencies of the absorption line maxima are plotted by symbols is panels (c) and (f). The solid lines show model calculation results for the Frenkel exciton states, using the theoretical approach of Sec. V. The experimental data were fitted with the following parameters: $g_c^\zeta = 1.81$, $g_c^\epsilon = 1.25$, $\delta g_c = 0.30$ for the (c) panel and $g_a^\zeta = 1.93$, $g_a^\epsilon = 2.06$, $\delta g_a = -0.04$ for the (f) panel. The parameters $|t_F| = 0.06$ meV and $\Delta^\zeta = 0.5$ meV are the same for both panels.

the application of the magnetic field drastically modifies the absorption spectra. In the field range exceeding $B_0 = 1.4$ T, the linewidth is strongly reduced from about 0.5 meV down to about 0.06–0.14 meV. A fan of narrow lines becomes well resolved in which one can distinguish up to eight lines. This number is just the one that can be expected for the Davydov-split Frenkel excitons of the four 4*b* Cu^{2+} ions having the spin value $S = 1/2$ within the unit cell, as discussed in detail in Sec. V. The field evolution of the spectra can be nicely followed in the contour plot in Fig. 4(b). Here, a rather drastic transformation of the spectra above $B_0 = 1.4$ T is observed, while below this value a broad absorption band is found. In strong fields, the eight exciton lines grouped into four pairs with the same splitting $\Delta_D = 0.12$ meV within each pair are reliably resolved. The independence of the splitting of the field strength allows us to assign these lines to Davydov-split pairs.

In the field range below $B_0 = 1.4$ T, the behavior of the lines is complicated and no fine-structure can be resolved presumably because of broadening and overlapping of several lines due to the presence of several antiferromagnetic domains and correspondingly a not well-defined spin structure [4]. One can see in Fig. 4(c) that the four lowest-in-energy lines originate from the *A* line observed in zero field (see Fig. 3) so that we label them from A_1 to A_4, and the four upper lines are assigned to the zero-field *B* line and are labeled from B_5 to B_8. It is important to note that the two pairs of lines $A_{1,2}$ and $B_{5,6}$ have notably larger intensities than the two others. For instance, at $B = 5$ T the absorption coefficient of the stronger $A_{1,2}$ lines amounts to 20 cm^{-1}, whereas for the $A_{3,4}$ lines it is 5 cm^{-1} only. One can further see from the bottom row of panels in Fig. 4 that in the $\mathbf{B} \parallel a$ configuration the behavior is qualitatively similar. The critical field is also $B_0 = 1.4$ T, but the slopes of the line shifts with field are notably different. The second result is expected as the magnetic structure is anisotropic with the antiferromagnetic spins lying predominantly in the (*ab*) plane [4]. An understanding of the line structure and field shifts calls for a dedicated theory, which is presented in Sec. V.

The electronic excitations related to the ZP lines in $3d^n$ insulators should most adequately be regarded as Frenkel excitons as discussed in earlier literature [27–31,33,34,41–43]. However, the concept of Frenkel excitons can actually be applied only to those cases in which the absorption lines are narrow enough so that they can be well resolved in an applied magnetic field, at least at low temperature. The narrowness of the ZP absorption lines in CuB_2O_4 at $T = 1.6$ K provides just the right scenario for applying this concept. The observation of the zero-field splitting into the absorption line doublet and of the fine splitting in applied magnetic field at

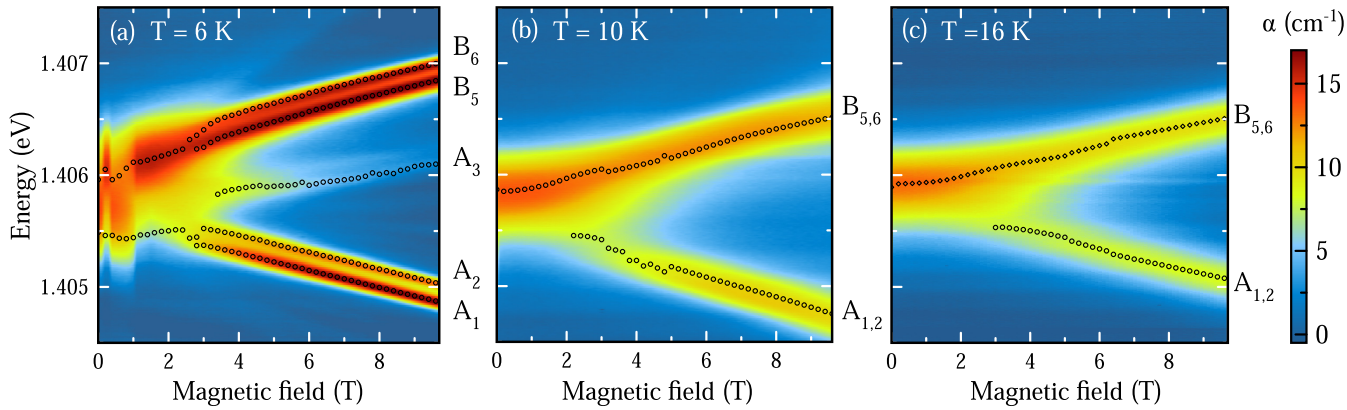

FIG. 5. Contour plots of exciton absorption spectra at $T =$ (a) 6 K, (b) 10 K, and (c) 16 K for the (101) sample. The π absorption spectra are shown in the configuration $\mathbf{E} \parallel c$, $\mathbf{k} \parallel b$, and $\mathbf{B} \parallel c$. Black symbols show the energies of the line maxima.

low temperature are very important features for the development of a theoretical model of the Frenkel excitons and their Davydov splitting in CuB_2O_4 which will be presented in Sec. V.

C. Temperature dependence of Frenkel excitons

An increase of temperature leads to a broadening of the exciton absorption lines and modifications of their splittings and magnetic field dependencies. Figure 5 shows contour plots of exciton π absorption spectra at $T = 6$ K [Fig. 5(a)], 10 K [Fig. 5(b)], and 16 K [Fig. 5(c)] ($\mathbf{E} \parallel c$, $\mathbf{k} \parallel b$) in the

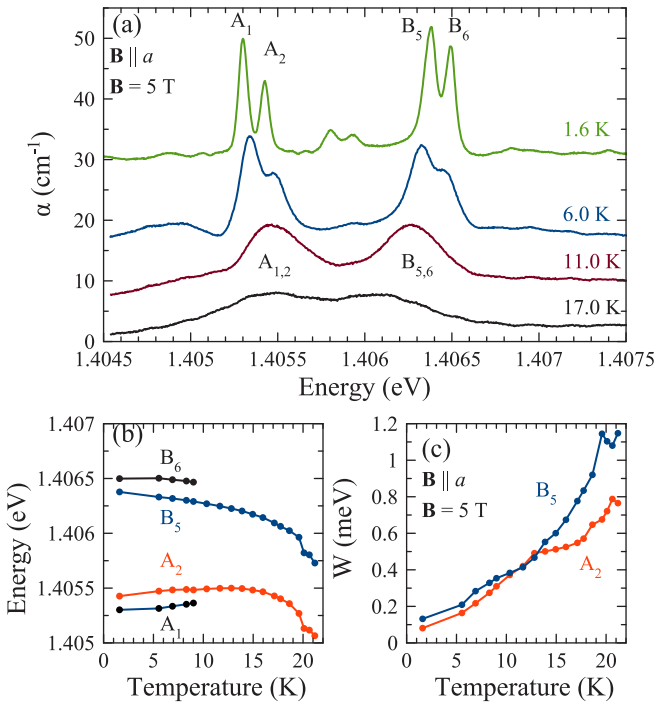

FIG. 6. (a) π-absorption spectra of CuB_2O_4 at $B = 5$ T in the $\mathbf{B} \parallel a$ geometry, measured at different temperatures for the (101) sample. (b) Spectral positions of the A_1, A_2, B_5, and B_6 exciton lines in dependence on temperature. (c) FWHM of the exciton lines with large amplitude in dependence on temperature.

$\mathbf{B} \parallel c$ configuration for the (101) sample. The spectral lines broaden so that separation of the eight exciton levels becomes complicated, but the doublet structure remains resolvable at $T = 6$ K. One can see that the critical field at which the spin splitting of the Frenkel excitons can be resolved is increased to $B_0 = 3$ T. For fields above this value the fitting procedure allows us to distinguish two doublets ($A_{1,2}$ and $B_{5,6}$) and the unresolved weak line $A_{3,4}$, the maxima of which are shown by the black symbols in Fig. 5(a). A further temperature increase leads to a smearing of the fine-structure so that only broad spectral lines are observed at 10 K [Fig. 5(b)] and 16 K [Fig. 5(c)].

A similar behavior is observed for the $\mathbf{B} \parallel a$ configuration. To illustrate this, we show in Fig. 6(a) an example of absorption spectra at $B_a = 5$ T, measured at various temperatures. The spectrum at $T = 1.6$ K consists of four doublets. Increasing the temperature to $T = 6$ K leads to line broadening and at $T > 9$ K the doublets cannot be resolved, but only two broad lines are distinguishable.

As was shown above, the exciton fine-structure depends on the mutual orientation of the external magnetic field and the crystal c axis. To obtain the parameters of all spectral lines shown in Figs. 4 and 5, each absorption spectrum at high magnetic fields ($B > 1.4$ T) was fitted by eight Lorentzian functions for $T = 1.6$ K and 6 K but only two Lorentzian

TABLE I. Magnetic field slopes β of the A_{1-4} and B_{5-8} groups of exciton lines, evaluated from the data for the $\mathbf{B} \parallel c$ and $\mathbf{B} \parallel a$ configurations, measured at different temperatures.

T (K)	A_1, A_2	A_3, A_4	B_5, B_6	B_7, B_8
		$\mathbf{B} \parallel c$		
1.6	−0.54	1.30	0.65	2.41
6.0	−0.78	1.24	1.08	
10.0	−0.99		0.88	
16.0	−0.86		0.72	
		$\mathbf{B} \parallel a$		
1.6	−0.94	0.92	1.07	2.98
6.0	−1.32	0.77	1.41	
10.0	−1.59		1.29	
16.0	−1.34		1.22	

TABLE II. Zero-field energy offsets $\mathbb{E}_0$ (eV) at different temperatures for the A_{1-4} and B_{5-8} exciton lines. The data are evaluated from the magnetic-field dependencies for the $\mathbf{B} \parallel c$ configuration.

T (K)	$A_{1,2}$	$A_{3,4}$	$B_{5,6}$	$B_{7,8}$
		$\mathbf{B} \parallel c$		
1.6	1.40561	1.40557	1.40616	1.40603
5.0	1.40568	1.40571	1.40613	
10.0	1.40564		1.40577	
16.0	1.40580		1.40585	

functions are used for $T > 9$ K. The spectral positions of A_1, A_2, B_5, and B_6 lines are shown in Fig. 6(b) as functions of temperature. The width of the exciton lines increases from 0.08 meV up to 0.8 meV for the A_1, A_2 doublet and from 0.13 meV up to 1.1 meV for the B_5, B_6 doublet by a temperature increase up to 21 K, see Fig. 6(c).

The energy shifts of the exciton lines in magnetic field are interpolated by linear functions to define the slopes β and the energy offsets $\mathbb{E}_0$ at $B = 0$:

$$\mathbb{E}(B) = \beta \mu_B B + \mathbb{E}_0, \tag{1}$$

where μ_B is the Bohr magneton.

The slopes β of the exciton lines for different field configurations and temperatures are given in Table I. The A and B groups consist of two sets of doublets split by the energy Δ_D, which does not depend on the magnetic field. The energy offsets $\mathbb{E}_0$ for different temperatures are collected in Table II.

V. THEORETICAL ANALYSIS OF FRENKEL EXCITONS IN CuB_2O_4

A. Concept of Frenkel excitons in CuB_2O_4

As discussed in Sec. IV A, the concept of Frenkel excitons was proven to be essential for understanding the optical spectra of antiferromagnetic insulators. In particular, Frenkel excitons play a major role in the absorption resulting from electronic transitions between $3d^n$ states. However, most experiments were performed and theoretical models were proposed for the chromium Cr^{3+} antiferromagnets in which transitions between $3d^3$ electronic states can take place. These are the chromium oxides Cr_2O_3 and the rare-earth (R) orthochromites $RCrO_3$ [27–31,33,34,41–43].

Before proceeding to the theoretical analysis of the Frenkel excitons in CuB_2O_4, we would like to point out similarities and differences between CuB_2O_4 and the Cr^{3+} antiferromagnetic insulators. As for similarities, the number of magnetic ions in the unit cell of CuB_2O_4 in the $4b$ subsystem and of the chromium crystals is the same, namely four. Thus, similarities of the experimental results may be expected. However, at zero magnetic field only two lines are observed for CuB_2O_4 instead of four lines in the Cr^{3+} antiferromagnets. When the magnetic field is applied, four pairs of lines are resolved in CuB_2O_4 at low temperature, resulting in a total of eight exciton lines (see the spectra in Sec. IV B). Similar results were obtained in second harmonic generation studies of CuB_2O_4 [15]. In contrast, only four lines are found in the Cr^{3+} antiferromagnets. These and other results on the magnetoabsorption in CuB_2O_4 require the development of a microscopic model of Frenkel excitons

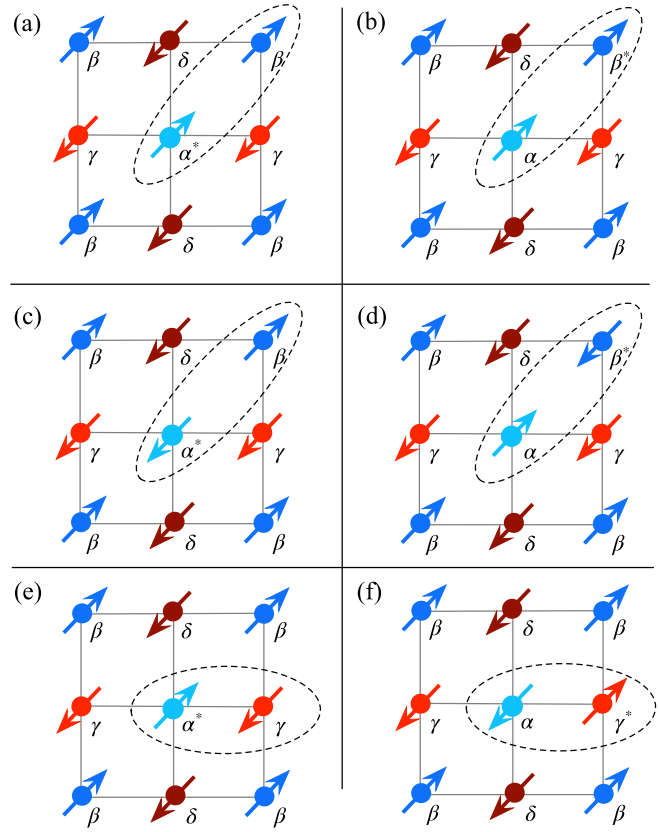

FIG. 7. Spin structures of CuB_2O_4 under optical excitation within a single antiferromagnetic sublattice and the opposite sublattice. The letters α, β, γ, and δ denote the Cu^{2+} ions at the four $4b$ positions within the single unit cell; the symbol * refers to the excited state. The pairs highlighted by dotted ovals in the (a) and (b) panels have the same excitation energy, even when the exchange interaction with the neighboring ions from the opposite sublattice is taken into account. Thus, resonant transfer of excitation is possible between the α and β Cu^{2+} ions within the same antiferromagnetic sublattice. Panels (c) and (d) show the spin structures under optical excitation accompanied by a spin flip. In this case, the resonant transfer of excitation accompanied by a spin flip is also possible. Panels (e) and (f) demonstrate the optical excitation of the α^* and γ^* Cu^{2+} ions from opposite antiferromagnetic sublattices when the excitation energy transfer is forbidden.

in this antiferromagnetic material. The model has to account for the spin states of the Cu^{2+} $4b$ ions and their role in the Davydov splitting of the Frenkel excitons. We use the cell perturbation method [28,29,31] for calculating the Frenkel exciton energies, which is performed in two steps.

The elementary unit cell of CuB_2O_4 contains four Cu^{2+} $4b$ ions, which are denoted as α, β, γ, and δ, see Figs. 1(a) and 7(a). The optical absorption in the 1.4055–1.4061 eV spectral range is due to the transitions from the ground state $|\epsilon\rangle = |x^2 - y^2\rangle$ of the Cu^{2+} ion to its excited state $|\zeta\rangle = |xy\rangle$ at the $4b$ position, see Fig. 1(b) [8]. Both these states are orbital singlets which are twofold spin $S = 1/2$ degenerate ($m_s = \pm 1/2$). In the ordered antiferromagnetic phase below T_N, the splitting of the ground state under the action of the exchange (molecular) field caused by the neighboring copper

spins is about 7.2 meV [13]. Therefore, it can be reasonably well assumed that at low temperatures only the lower $m_s = -1/2$ substate of the spin doublet is populated. The magnitude of the exchange splitting of the excited state is not known, and its determination is one of the goals of our theory.

Other important goals to clarify are the particular features of the exciton states and the parameter of the energy transfer of resonant excitation between the four Cu^{2+} ions occupying the α, β, γ, and δ positions within the elementary unit cell. Since the wavelength corresponding to optical absorption is much larger than the lattice period, in accordance with the law of momentum conservation, exciton transitions with only small values of the wave vector $\mathbf{q}$ can be excited and probed optically. The problem of calculating $q = 0$ states is thus reduced to the diagonalization of the interaction energy between the α, β, γ, and δ ions within the basis of wave functions belonging to a single unit cell.

These wave functions can be written in the following form:

$$\begin{aligned}
|\psi_1\rangle &= |\zeta_\alpha+\rangle|\epsilon_\beta+\rangle|\epsilon_\gamma-\rangle|\epsilon_\delta-\rangle,\\
|\psi_2\rangle &= |\zeta_\alpha-\rangle|\epsilon_\beta+\rangle|\epsilon_\gamma-\rangle|\epsilon_\delta-\rangle,\\
|\psi_3\rangle &= |\epsilon_\alpha+\rangle|\zeta_\beta+\rangle|\epsilon_\gamma-\rangle|\epsilon_\delta-\rangle,\\
|\psi_4\rangle &= |\epsilon_\alpha+\rangle|\zeta_\beta-\rangle|\epsilon_\gamma-\rangle|\epsilon_\delta-\rangle,\\
|\psi_5\rangle &= |\epsilon_\alpha+\rangle|\epsilon_\beta+\rangle|\zeta_\gamma+\rangle|\epsilon_\delta-\rangle,\\
|\psi_6\rangle &= |\epsilon_\alpha+\rangle|\epsilon_\beta+\rangle|\zeta_\gamma-\rangle|\epsilon_\delta-\rangle,\\
|\psi_7\rangle &= |\epsilon_\alpha+\rangle|\epsilon_\beta+\rangle|\epsilon_\gamma-\rangle|\zeta_\delta+\rangle,\\
|\psi_8\rangle &= |\epsilon_\alpha+\rangle|\epsilon_\beta+\rangle|\epsilon_\gamma-\rangle|\zeta_\delta-\rangle. \qquad (2)
\end{aligned}$$

To shorten the notation of these wave functions, we use below the following notations:

$$|\zeta_\alpha\sigma_\zeta\rangle, \quad |\zeta_\beta\sigma_\zeta\rangle, \quad |\zeta_\gamma\sigma_\zeta\rangle, \quad |\zeta_\delta\sigma_\zeta\rangle, \qquad (3)$$

where $\sigma_\zeta = \pm 1/2$ are the spin quantum numbers in the excited state.

B. Resonant energy transfer in the system of exchange-coupled spins

We define the superexchange interaction between the neighboring copper ions through intermediate boron-oxygen tetrahedrons [2] in the form $H_{\rm ex} = J_{\alpha,\gamma}(\mathbf{S}_\alpha\mathbf{S}_\gamma)$, where $J_{\epsilon,\epsilon} = J_{\alpha,\gamma} = J_{\alpha,\delta} = J_{\beta,\gamma} = J_{\beta,\delta} = 3.85$ meV [5,44]. Since the wave functions of the ground and excited states are orthogonal to each other, then according to the Goodenough-Kanamori-Anderson rules one expects that the exchange interaction between the ground $|\epsilon\rangle = |x^2 - y^2\rangle$ state of a single Cu^{2+} ion and the excited state $|\zeta\rangle = |xy\rangle$ state of another neighboring Cu^{2+} ions has ferromagnetic character, that is, $J_{\zeta,\epsilon} = J_{\alpha^*,\gamma} = J_{\alpha^*,\delta} = J_{\beta^*,\delta} = J_{\beta^*,\gamma} \leqslant 0$. Here the index $*$ marks the excited state.

Various cases of the influence of spin ordering on the transfer of excitation energy between the Cu^{2+} ions are explained in Fig. 7. A pair of Cu^{2+} ions at the α and β positions within the same antiferromagnetic sublattice is considered in Figs. 7(a) and 7(b). Figure 7(a) shows a case when under optical excitation the α ion moves into the α^* excited state $|\zeta\rangle = |xy\rangle$ with conservation of the spin orientation, while the β ion stays in the ground $|\epsilon\rangle = |x^2 - y^2\rangle$ state. In Fig. 7(b) the case is inverted — the α ion stays in the ground state, whereas the β^* ion moves into the excited state. The optical excitation energies of the discussed pair, taking into account also the nearest Cu^{2+} ions, are the same in both cases shown in Figs. 7(a) and 7(b), i.e., $E_{\rm ex}(a) = E_{\rm ex}(b)$:

$$\begin{aligned}
E_{\rm ex}(a) &= -2\tfrac{1}{4}J_{\alpha^*,\gamma} - 2\tfrac{1}{4}J_{\alpha^*,\delta} - 2\tfrac{1}{4}J_{\beta,\gamma} - 2\tfrac{1}{4}J_{\beta,\delta}\\
&= -J_{\epsilon,\epsilon} - J_{\zeta,\epsilon}. \qquad (4)
\end{aligned}$$

Thus, the equality condition for the excitation energies of Cu^{2+} ions at the α and β positions is not violated. Similarly, one can verify that the above condition remains valid also under optical excitation accompanied by a spin flip because in this case the pair energy is equal to

$$E_{\rm ex}(c) = E_{\rm ex}(d) = J_{\zeta,\epsilon} - J_{\epsilon,\epsilon}. \qquad (5)$$

Here, $E_{\rm ex}(c)$ and $E_{\rm ex}(d)$ are the optical excitation energies for the configurations shown in Figs. 7(c) and 7(d), respectively.

Let us now discuss the processes of optical excitation when the exchange interaction between ions from opposite antiferromagnetic sublattices is included. Figures 7(e) and 7(f) demonstrate an example of a pair of ions at the α and γ positions. Similar to the previous case, α, γ and α^*, γ^* mark the Cu^{2+} ions in the ground and excited states, respectively. The exchange interaction energy between the spins for the two configurations shown in Figs. 7(e) and 7(f) can be written as

$$E_{\rm ex}(e) = -\tfrac{3}{4}J_{\gamma,\beta} - \tfrac{3}{4}J_{\alpha^*,\delta} - \tfrac{1}{4}J_{\alpha^*,\gamma}, \qquad (6)$$

$$E_{\rm ex}(f) = \tfrac{3}{4}J_{\gamma,\beta} + \tfrac{3}{4}J_{\alpha^*,\delta} - \tfrac{1}{4}J_{\alpha^*,\gamma}, \qquad (7)$$

where $E_{\rm ex}(e)$ and $E_{\rm ex}(f)$ are the optical excitation energies for the two configurations shown in Figs. 7(e) and 7(f), respectively. One can see that the energies in these two cases are different and, therefore, the necessary condition for a resonant transfer of excitation is violated. Thus, we come to the conclusion that a substantial resonant excitation transfer occurs only within each of the two opposite antiferromagnetic sublattices. It should be noted that this important conclusion had not been established in previous publications. The exchange interaction causes the splitting of the ground and excited states and optical excitation energies change.

C. Davydov splitting of Frenkel excitons

Next, we move on to the discussion of the interaction of the excited state of the Cu^{2+} ion with the surrounding Cu^{2+} ions in terms of the molecular field approximation. For the $Cu^{2+}(\alpha^*)$ ion, the molecular field operator has the form $\hat{H}_{\rm mol} = 2\mu_{\rm B}\mathbf{S}_{\alpha^*}\mathbf{M}_\alpha$ in which the exchange field $\mathbf{M}_\alpha$ is considered as a fitting parameter. It can be seen from Figs. 7(a) or 7(b) that $H_{\rm mol}(\alpha^*) = H_{\rm mol}(\beta^*) = -J_{\zeta,\epsilon}$, but, for example, in Fig. 7(f), $H_{\rm mol}(\gamma^*) = J_{\zeta,\epsilon}$, i.e., the exchange interaction of the excited state with the surrounding spins is different for different positions in the unit cell and therefore it has to be taken into account.

Let us further consider the mechanisms of the excitation energy transfer from one Cu^{2+} ion to another using as an example the α and β pair of ions. The energies of the states with the wave functions $\alpha^+_{\zeta\sigma}\beta^+_{\epsilon\sigma}|0\rangle$ and $\alpha^+_{\epsilon\sigma}\beta^+_{\zeta\sigma}|0\rangle$ are equal. The Frenkel-Davydov integral of the excitation transfer is

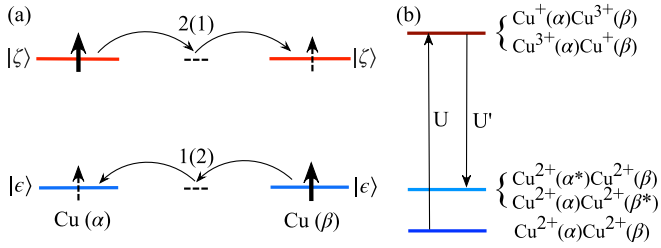

FIG. 8. (a) Illustration of the excitation transfer mechanism caused by an electron hopping from one Cu^{2+} ion to another through the intermediate tetrahedral BO_4 groups [2] shown schematically by the dashed lines. Thick and dashed vertical arrows show the initial and final positions for spin hopping. (b) Energy level diagram for deriving the operator of the excitation transfer between the $[Cu^{2+}(\alpha)\,Cu^{2+}(\beta)]$ and $[Cu^{2+}(\alpha^*)\,Cu^{2+}(\beta)]$ or $[Cu^{2+}(\alpha)\,Cu^{2+}(\beta^*)]$ states through the $[Cu^{+}(\alpha)\,Cu^{3+}(\beta)]$ or $[Cu^{3+}(\alpha)\,Cu^{+}(\beta)]$ states.

determined by the equation

$$t_{\rm F}^{(1)} = \langle\epsilon_\alpha(\mathbf{r}_1)\zeta_\beta(\mathbf{r}_2)|V(\mathbf{r}_1-\mathbf{R}_{\alpha,\beta}-\mathbf{r}_2)|\zeta_\alpha(\mathbf{r}_1)\epsilon_\beta(\mathbf{r}_2)\rangle - \langle\epsilon_\alpha(\mathbf{r}_1)\zeta_\beta(\mathbf{r}_2)|V(\mathbf{r}_1-\mathbf{R}_{\alpha,\beta}-\mathbf{r}_2)|\zeta_\alpha(\mathbf{r}_2)\epsilon_\beta(\mathbf{r}_1)\rangle, \quad (8)$$

where $V(\mathbf{r}_1-\mathbf{R}_{\alpha,\beta}-\mathbf{r}_2)$ is the Coulomb interaction of the electrons, $\mathbf{R}_{\alpha,\beta}$ is the radius-vector between the α and β positions, and $\mathbf{r}_1$ and $\mathbf{r}_2$ are taken from these two positions, respectively. The first term in this equation is the Coulomb two-center integral and the second one is the exchange integral.

Figure 8(a) shows a sketch of the excitation transfer from one Cu^{2+} ion to another. The numbers 1(2) and 2(1) denote the cascaded hopping of electrons between the order of Cu^{2+} ions through the intermediate tetrahedral BO_4 groups [2]. The matrix elements describing the electron hopping between the ground and excited states are

$$t_{\epsilon\epsilon} = \langle\epsilon(\mathbf{r}-\mathbf{R}_\alpha)|\frac{p^2}{2m}+V|\epsilon(\mathbf{r}-\mathbf{R}_\beta)\rangle, \quad (9)$$

$$t_{\zeta\zeta} = \langle\zeta(\mathbf{r}-\mathbf{R}_\alpha)|\frac{p^2}{2m}+V|\zeta(\mathbf{r}-\mathbf{R}_\beta)\rangle. \quad (10)$$

Here $\mathbf{r}$ is the variable for integration over space, $\mathbf{R}_\alpha$ and $\mathbf{R}_\beta$ are the radius vectors to the Cu^{2+} ion in the α and β positions, respectively, p is the momentum of the electron, and m is the electron mass. These equations show that the matrix elements include the kinetic energy operator and that the ground and excited states are independent of the spin variables. In this regard, by analogy with the Anderson theory of superexchange interaction, this mechanism of excitation transfer can be classified as kinetic [45]. The energy of the electron transfer from one Cu^{2+} ion to another is $E = 5.9$ eV [45] and it is larger than the optical excitation energy $E = 1.40575$ eV. Therefore, in the second order of perturbation theory we obtain the following equation for the transfer integral:

$$t_F^{(2)} = \left[\frac{1}{U}+\frac{1}{U'}\right]t_{\epsilon\epsilon}t_{\zeta\zeta}. \quad (11)$$

Here U is the transfer energy of an electron from the $Cu^{2+}(\alpha)$ state to the $[Cu^{+}(\alpha)\ Cu^{3+}(\beta)]$ state and U' is the transfer energy of an electron from the $[Cu^{+}(\alpha)\ Cu^{3+}(\beta)]$ state to $Cu^{2+}(\alpha^*)$. The electron transfer between the $Cu^{2+}(\beta)$ and $Cu^{2+}(\beta^*)$ states through the $[Cu^{3+}(\alpha)\ Cu^{+}(\beta)]$ state can be described by the U and U' energies. An explanatory diagram of the virtual excitations is shown in Fig. 8(b). When deriving Eq. (11), we assume that $U - U' \ll U$.

Taking into account the spatial distribution of the phases of the involved wave functions of the ground $|\epsilon_a\rangle$ and excited $|\zeta_a\rangle$ states, one can ensure that the product $t_{\epsilon\epsilon}t_{\zeta\zeta} < 0$. The total transfer integral $t_F = t_F^{(1)} + t_F^{(2)}$ is considered as an adjustable parameter, which is determined from the experimental data. The $t_F^{(1)}$ value calculated using the Hartree-Fock wave functions of the $Cu^{2+}(3d^9)$ ion is about -6×10^{-6} meV. Since the absolute value of $t_{\rm F} = 0.06$ meV determined from the experimental data turns out to be much larger than the calculated value, we conclude that $t_F^{(2)} < 0$ plays the dominant role and thus the total $t_F < 0$. The Davydov splitting defined from experiment is equal to $\Delta_D = 2t_{\rm F}$.

D. Frenkel excitons in an applied magnetic field

The interaction of the magnetic Cu^{2+} ions ($S = 1/2$) with an applied magnetic field results in the Zeeman splitting of the ground $|\epsilon\rangle$ and excited $|\zeta\rangle$ states (we remind that $S = 1/2$ in both these states) and the resulting splitting is described in the usual way by operators of the form

$$\hat{H}_Z^{\epsilon(\zeta)} = \mu_{\rm B} g_l^{\epsilon(\zeta)} S_l^{\epsilon(\zeta)} B_l. \quad (12)$$

Here, $\mu_{\rm B}$ is the Bohr magneton, the indices $l = (a, b, c)$ define the crystallographic axes, $g_l^{\epsilon(\zeta)}$ is the effective g-factor of the Cu^{2+} ion which depends on the magnetic susceptibility tensor χ_{ll}, and B_l is the applied magnetic field.

The energy matrix in the basis of the ψ_i ($i = 1-8$) states from Eq. (2) has the following nonzero elements for the $\mathbf{B} \parallel a$ geometry:

$$H(1,1) = -\Delta^\zeta/2 + \mu_{\rm B}\left(g_a^\zeta - g_a^\epsilon\right)H_a/2, \quad (13)$$

$$H(2,2) = -\Delta^\zeta/2 - \mu_{\rm B}\left(g_a^\zeta + g_a^\epsilon\right)H_a/2, \quad (14)$$

$$H(3,3) = H(1,1), \quad (15)$$

$$H(4,4) = H(2,2), \quad (16)$$

$$H(5,5) = \Delta^\zeta/2 + \mu_{\rm B}\left(g_a^\zeta + g_a^\epsilon\right)H_a/2, \quad (17)$$

$$H(6,6) = \Delta^\zeta/2 - \mu_{\rm B}\left(g_a^\zeta - g_a^\epsilon\right)H_a/2, \quad (18)$$

$$H(7,7) = H(5,5), \quad (19)$$

$$H(8,8) = H(6,6), \quad (20)$$

$$H(1,3) = H(2,4) = H(5,7) = H(6,8) = t_{\rm F}. \quad (21)$$

The spin quantization axis is chosen along the applied magnetic field H_a, $B_a = (1 + 4\pi\chi_{aa})H_a$ is the magnetic induction component and χ_{aa} is the magnetic susceptibility tensor component. For describing the experimental data, the values $g_{\rm a}^\zeta$ and $g_{\rm a}^\epsilon$, which include the $(1 + 4\pi\chi_{aa})$ term, are considered as fitting parameters. It is assumed that they do not vary across the entire range of magnetic fields. In the case of $\mathbf{H} \parallel c$, the a index should be replaced by the c index in the matrix elements. The diagonalization of the $H(i, j)$ matrix makes it possible to find the relative position of the exciton energy levels while the average energy value remains the same when summing over all states as in the absence of the magnetic field.

For obtaining the energies of the optical transitions, the difference $E(\zeta) - E(\epsilon) + \Delta_l^\epsilon$ should be added to all diagonal elements of the $H(i, j)$ matrix. Here, the quantity $\Delta_l^\epsilon = \mu_B(1/2 g_l^\epsilon + \delta g_l)B_l$ takes into account the energy decrease of the lowest Zeeman component of the copper ion in the ground state from which the optical transitions occur. The δg_l is an additional parameter introduced for better fitting results, whose origin is, however, not clear. The energy $E(\zeta) - E(\epsilon) = 1.40556$ eV is due to the action of the crystal and exchange fields, as well as the spin-orbit interaction, on the Cu^{2+} $4b$ ion at zero magnetic field.

VI. MODELING OF EXPERIMENTAL RESULTS

In this section, we use the developed theory for describing our experimental results on the Frenkel excitons in magnetic field. The modeling allows us to evaluate the exciton parameters which determine the energy spectra and their modification with increasing magnetic field. The best fits to the experimental data at $T = 1.6$ K are shown by the lines in Figs. 4(c) and 4(f). The fit parameters are given in the figure caption and also in Table III. Only five parameters are used for the fitting, but they are related to different properties of the exciton structure and, therefore, each of them can be evaluated with high accuracy. The splitting $\Delta^\zeta = 0.50$ meV between the A and B broad lines in zero magnetic field is due to the exchange interaction of the excited state of the Cu^{2+} ion with the surrounding Cu^{2+} ions from both the $4b$ and $8d$ subsystems. The Davydov splitting of $\Delta_D = 0.12$ meV within each doublet is independent of the magnetic field and provides the transfer integral value of $t_F = \Delta_D/2 = 0.06$ meV. The slopes of the four doublets in magnetic field give the g-factors of the ground (g^ϵ) and excited (g^ζ) states and also the additional spectral shift of all spectral lines due to the splitting of the ground state Δ_l^ϵ. The parameter Δ_l^ϵ is responsible for the shift of the center of gravity of the two A and B doublet sets.

We perform fits for all sets of experimental data for the two field configurations and the four temperatures which were presented above. For the evaluation it is worthwhile to give the equations for the slopes of the exciton lines in magnetic field which are determined by the g-factors in the ground and excited states and the additional correction factor δg_l. One can define the g-factors from the slopes of the spectral lines given in Table I

$$\beta(A_{1,2}) = \delta g_l - g_l^\zeta/2, \tag{22}$$

$$\beta(A_{3,4}) = \delta g_l + g_l^\zeta/2, \tag{23}$$

$$\beta(B_{5,6}) = \delta g_l - g_l^\zeta/2 + g_l^\epsilon, \tag{24}$$

$$\beta(B_{7,8}) = \delta g_l + g_l^\zeta/2 + g_l^\epsilon. \tag{25}$$

The evaluated experimental values Δ^ζ, t_F, and the calculated parameters g^ϵ, g^ζ, and δg are collected in Table III. We conclude from the presented data that a temperature increase up to $T = 10$ K does not change the splitting Δ^ζ due to the exchange interaction with the surrounding copper ions. However, the Davydov splitting $\Delta_D = 2t_F$ is increased by a factor of 1.5 and 1.3 for the $\mathbf{B} \parallel c$ and $\mathbf{B} \parallel a$ geometry, respectively. In parallel, the g-factors of the ground and excited states are increased approximately by a value of 0.6. The additional δg parameter changes with temperature. A further increase of the temperature complicates the determination of the Davydov splitting since the line widths increase considerably leading to only two merged broad bands from the eight narrow exciton lines. To determine the g-factor in the excited state, knowledge of the slope of at least three exciton line pairs is required allowing one to solve Eqs. (22) to (25) with the three unknown variables g^ϵ, g^ζ, and δg. From $T = 10$ K upwards, only g^ϵ can be calculated. g^ϵ changes between 1.86 and 1.58 for $\mathbf{B} \parallel c$ and 2.88 and 2.56 for $\mathbf{B} \parallel a$. The parameter Δ^ζ stays constant but decreases to $\Delta^\zeta = 0.4$ meV at $T = 16$ K. In addition to the parameters of the Frenkel excitons extracted from the model calculations, it is also necessary to comment on the different intensities of the spectral lines observed in the experiment. The intensity of the spectral lines is determined by the ED or MD character of the exciton transition. Therefore, we calculated the wave functions of the $q = 0$ exciton states having energies when $B = 8$ T is applied, they are collected in Table IV. We note that the wave functions keep the same form for $B > 1.6$ T when CuB_2O_4 is in the commensurate phase [4]. The wave functions are given for the exciton bands in the crystal structure with an inversion center. In this case, a set of purely symmetric (upper energy component of the doublets) and purely antisymmetric (lower component) exciton states should be observed. Considering that the lowest (A_1) state is symmetric, we come to the conclusion that the optical

TABLE III. Experimental parameters Δ^ζ, t_F and calculated values of g^ϵ, g^ζ, and δg at different temperatures in the $\mathbf{B} \parallel c$ and $\mathbf{B} \parallel a$ configurations.

T (K)	Δ^ζ (meV)	t_F (meV)	g_l^ϵ	g_l^ζ	δg_l
		$\mathbf{B} \parallel c$			
1.6	0.50	0.06	1.25	1.81	0.30
6.0	0.50	0.09	1.86	2.02	0.23
10.0	0.50		1.87		
16.0	0.40		1.58		
		$\mathbf{B} \parallel a$			
1.6	0.50	0.06	2.06	1.93	−0.04
6.0	0.50	0.08	2.73	2.09	−0.28
10.0	0.50		2.88		
16.0	0.40		2.56		

TABLE IV. Wave functions ψ_i of the Frenkel exciton states X with the wave vector $q = 0$ excited by photons with energy E_X at $B = 8$ T for the $\mathbf{B} \parallel a$ geometry.

X	E_X (eV)	Wave functions ψ_i
A_1	1.40510	$(\lvert\zeta_\alpha-\rangle + \lvert\zeta_\beta-\rangle)/\sqrt{2}$
A_2	1.40520	$(\lvert\zeta_\alpha-\rangle - \lvert\zeta_\beta-\rangle)/\sqrt{2}$
A_3	1.40600	$(\lvert\zeta_\alpha+\rangle + \lvert\zeta_\beta+\rangle)/\sqrt{2}$
A_4	1.40610	$(\lvert\zeta_\alpha+\rangle - \lvert\zeta_\beta+\rangle)/\sqrt{2}$
B_5	1.40656	$(\lvert\zeta_\gamma-\rangle + \lvert\zeta_\delta-\rangle)/\sqrt{2}$
B_6	1.40666	$(\lvert\zeta_\gamma-\rangle - \lvert\zeta_\delta-\rangle)/\sqrt{2}$
B_7	1.40745	$(\lvert\zeta_\gamma+\rangle + \lvert\zeta_\delta+\rangle)/\sqrt{2}$
B_8	1.40755	$(\lvert\zeta_\gamma+\rangle - \lvert\zeta_\delta+\rangle)/\sqrt{2}$

transitions to the upper doublet components have ED character, while the lower ones have MD character. Note that if the sign of the exchange field in the excited state is inverted, then the symmetric and antisymmetric states in the doublets swap their energies. We emphasize that the actual crystal structure of CuB_2O_4 is noncentrosymmetric (point group $-42m$) and, therefore, the absorption lines observed in the experiments might have mixed ED-MD character.

VII. CONCLUSION

We carried out a detailed experimental study of the polarized magnetoabsorption on the $4b$ subsystem of the Cu^{2+} ions in the antiferromagnet CuB_2O_4, for which we used optical spectroscopy with high spectral resolution in strong magnetic fields up to 9.5 T across the temperature range from $T = 1.6$ K up to the antiferromagnetic-paramagnetic phase transition at $T_N = 20$ K. The study was performed around the lowest-in-energy electronic transition between the orbitally nondegenerate ground $|\epsilon\rangle = |x^2 - y^2\rangle$ and excited $|\zeta\rangle = |xy\rangle$ states of the Cu^{2+} ion in the spectral range of 1.4055–1.4065 eV. Though this transition was previously studied in several publications cited in the introductory Sec. I, our approach using high spectral resolution and applying magnetic field allowed us to obtain unexpected results. At the lowest temperature $T = 1.6$ K, only a doublet of broad lines with a partially resolved splitting of 0.50 meV was observed at zero magnetic field. This splitting is surprising because the involved electronic transition takes place between orbitally nondegenerate states. It was assumed earlier in Ref. [22] that the doublet structure is due to the Davydov splitting originating from the presence of the two Cu^{2+} $4b$ ions in the primitive unit cell of CuB_2O_4. However, above the critical magnetic field of $B_0 = 1.4$ T we discovered a well-resolved splitting of the zero-field doublet into a fan of eight narrow lines and these observations required a revision of the assumption put forward in Ref. [22] by raising the question about the origin of the observed level structure of Frenkel excitons subject to Zeeman and Davydov splitting. Moreover, our results showed that the Davydov splitting of the Frenkel excitons in CuB_2O_4 is drastically different from that reported inprevious studies in the Cr^{3+}-based antiferromagnets in which only the expected set of Frenkel excitons was observed, only partly as discussed in Sec. I.

The theoretical model developed in the present paper is based on a consistent analysis of the crystallographic and magnetic symmetry of the commensurate antiferromagnetic structure of the $4b$ spin Cu^{2+} subsystem and the exchange interactions within the $4b$ subsystem as well as with the $8d$ subsystem with oppositely oriented spins. As a result, the theoretical model allowed a convincing confirmation of the experimentally observed Zeeman and Davydov splitting of Frenkel excitons. Within the framework of the developed theory, reasonable values of the underlying parameters were obtained such as the exchange splitting $\Delta^{\zeta} = 0.5$ meV of the excited state, the Davydov splitting of $\Delta_D = 2t_F = 0.12$ meV, where t_F is the integral of the excitation transfer between the Cu^{2+} ions within the unit cell, as well as the g factors of the ground and excited states of the Cu^{2+} $4b$ ions, including the g-factor anisotropy. Our combined experimental and theoretical approach applied for solving complex exciton spectra in CuB_2O_4 can be also used in studies of other antiferromagnets in which Frenkel excitons decisively contribute to their optical spectra.

ACKNOWLEDGMENTS

This work was supported by the Deutsche Forschungsgemeinschaft via the International Collaborative Research Centre TRR 160 (Projects No. B2 and No. C8). The contribution of R.V.P. to this work was supported by Russian Foundation for Basic Research, Project No. 19-52-12063. The theoretical work of M.V.E. and A.R.N. was supported by the Russian Science Foundation, Project No. 19-12-00244.

[1] D. I. Mendeleev, *The Principles of Chemistry* (Saint Petersburg, 1900).

[2] M. Martinez-Ripoll, S. Martinez-Carrera, and S. Garcia-Blanco, The crystal structure of copper metaborate CuB_2O_4, Acta Cryst. B **27**, 677 (1971).

[3] G. K. Abdullaev and K. S. Mamedov, Refined crystal structure of copper metaborate CuB_2O_4, J. Struct. Chem. **22**, 637 (1981).

[4] A. E. Petrova and A. I. Pankrats, Copper metaborate CuB_2O_4 phase diagrams based on the results of measuring the magnetic moment, J. Exp. Theor. Phys. **126**, 506 (2018).

[5] M. Boehm, B. Roessli, J. Schefer, A. S. Wills, B. Ouladdiaf, E. Lelièvre-Berna, U. Staub, and G. A. Petrakovskii, Complex magnetic ground state of CuB_2O_4, Phys. Rev. B **68**, 024405 (2003).

[6] T. Kawamata, N. Sugawara, S. M. Haider, and T. Adachi, Thermal conductivity and magnetic phase diagram of CuB_2O_4, J. Phys. Soc. Jpn. **88**, 114708 (2019).

[7] R. V. Pisarev, I. Sänger, G. A. Petrakovskii, and M. Fiebig, Magnetic-Field Induced Second Harmonic Generation in CuB_2O_4, Phys. Rev. Lett. **93**, 037204 (2004).

[8] R. V. Pisarev, A. M. Kalashnikova, O. Schöps, and L. N. Bezmaternykh, Electronic transitions and genuine crystal-field parameters in copper metaborate CuB_2O_4, Phys. Rev. B **84**, 075160 (2011).

[9] M. Fiebig, I. Sänger, and R. V. Pisarev, Magnetic phase diagram of CuB_2O_4, J. Appl. Phys. **93**, 6960 (2003).

[10] M. Saito, K. Taniguchi, and T.-H. Arima, Gigantic optical magnetoelectric effect in CuB_2O_4, J. Phys. Soc. Jpn. **77**, 013705 (2008).

[11] S. Toyoda, N. Abe, S. Kimura, Y. H. Matsuda, T. Nomura, A. Ikeda, S. Takeyama, and T. Arima, One-Way Transparency of Light in Multiferroic CuB_2O_4, Phys. Rev. Lett. **115**, 267207 (2015).

[12] S. Toyoda, N. N. Abe, and T. Arima, Nonreciprocal Second Harmonic Generation in a Magnetoelectric Material, Phys. Rev. Lett. **123**, 077401 (2019).

[13] S. Toyoda, N. Abe, and T. Arima, Gigantic directional asymmetry of luminescence in multiferroic CuB_2O_4, Phys. Rev. B **93**, 201109(R) (2016).

[14] D. Kudlacik, V. Y. Ivanov, D. R. Yakovlev, V. F. Sapega, J. J. Schindler, J. Debus, M. Bayer, and R. V. Pisarev, Exciton

and exciton-magnon photoluminescence in the antiferromagnet CuB_2O_4, Phys. Rev. B **102**, 035128 (2020).

[15] J. Mund, D. R. Yakovlev, A. N. Poddubny, R. M. Dubrovin, M. Bayer, and R. V. Pisarev, Toroidal nonreciprocity of optical second harmonic generation, Phys. Rev. B **103**, L180410 (2021).

[16] S. Toyoda, M. Fiebig, T. Arima, Y. Tokura, and N. Ogawa, Nonreciprocal second harmonic generation in a magnetoelectric material, Sci. Adv. **7**, eabe2793 (2021).

[17] T. Arima, Magneto-electric optics in non-centrosymmetric ferromagnets, J. Phys.: Condens. Matter **20**, 434211 (2008).

[18] T. Arima and M. Saito, Comment on 'calculated chiral and magneto-electric dichroic signals for copper metaborate (CuB_2O_4) in an applied magnetic field,' J. Phys.: Condens. Matter **21**, 498001 (2009).

[19] S. W. Lovesey and U. Staub, Calculated chiral and magneto-electric dichroic signals for copper metaborate (CuB_2O_4) in an applied magnetic field, J. Phys.: Condens. Matter **21**, 142201 (2009).

[20] S. W. Lovesey and U. Staub, Reply to comment on 'calculated chiral and magneto-electric dichroic signals for copper metaborate (CuB_2O_4) in an applied magnetic field,' J. Phys.: Condens. Matter **21**, 498002 (2009).

[21] A. I. Nikitchenko and R. V. Pisarev, Magnetic and antiferromagnetic nonreciprocity of light propagation in magnetoelectric CuB_2O_4, Phys. Rev. B **104**, 184108 (2021).

[22] K. N. Boldyrev, R. V. Pisarev, L. N. Bezmaternykh, and M. N. Popova, Antiferromagnetic Dichroism in a Complex Multisublattice Magnetoelectric CuB_2O_4, Phys. Rev. Lett. **114**, 247210 (2015).

[23] J. Frenkel, On the transformation of light into heat in solids (i), Phys. Rev. **37**, 17 (1931).

[24] J. Frenkel, On the transformation of light into heat in solids (ii), Phys. Rev. **37**, 1276 (1931).

[25] A. S. Davydov, The theory of molecular excitons, Phys. Usp. **7**, 145 (1964).

[26] A. S. Davydov, *Theory of Molecular Excitons* (Plenum, New York, 1971).

[27] R. Loudon, Theory of infra-red and optical spectra of antiferromagnets, Adv. Phys. **17**, 243 (1968).

[28] J. P. van der Ziel, Optical spectrum of antiferromagnetic Cr_2O_3, Phys. Rev. **161**, 483 (1967).

[29] K. Aoyagi, K. Tsushima, and S. Sugano, Direct observation of Davydov splitting in antiferromagnetic $YCrO_3$, Solid State Commun. **7**, 229 (1969).

[30] R. S. Meltzer, M. Y. Chen, D. S. McClure, and M. Lowepari, Exciton-Magnon Bound State in MnF_2 and the Exciton Dispersion in MnF_2 and $RbMnF_3$, Phys. Rev. Lett. **21**, 913 (1968).

[31] J. W. Allen, R. M. Macfarlane, and R. L. White, Magnetic Davydov splittings in the optical absorption spectrum of Cr_2O_3, Phys. Rev. **179**, 523 (1969).

[32] J. Allen, Reinterpretation of $^4A_2 \rightarrow {}^2E$ exciton spectra in $YCrO_3$, Solid State Commun. **8**, 53 (1970).

[33] R. S. Meltzer, Davydov splitting in the optical absorption spectra of the $Cr^{+3}\,{}^2E$ state in some rare-earth orthochromites, Phys. Rev. B **2**, 2398 (1970).

[34] S. Sugano, K. Aoyagi, and K. Tsushima, Exciton absorption lines in antiferromagnetic rare-earth orthochromites – with particular reference to $YCrO_3^-$, J. Phys. Soc. Jpn. **31**, 706 (1971).

[35] R. D. Mero, C.-H. Lai, C.-H. Du, and H.-L. Liu, Spectroscopic Signature of Spin-Charge-Lattice Coupling in CuB_2O_4, J. Phys. Chem. C **125**, 4322 (2021).

[36] G. A. Petrakovskii, K. A. Sablina, D. A. Velikanov, A. Vorotynov, N. V. Volkov, and A. F. Bovina, Synthesis and magnetic properties of copper metaborate single crystals, CuB_2O_4, Cryst. Rep. **45**, 853 (2000).

[37] D. S. McClure, in *Electronic Spectra of Molecules and Ions in Crystals Part II. Spectra of Ions in Crystals: Part II. Spectra of Ions in Crystals*, edited by F. Seitz and D. Turnbull, Solid State Physics (Academic Press, New York, 1959), Vol. 9, pp. 399–525.

[38] M. V. Eremin, On the theory of magnetoelectric coupling in $LiCu_2O_2$, J. Exp. Theor. Phys. **6**, 990 (2019).

[39] A. Abragam and B. Bleaney, *Electron Paramagnetic Resonance of Transition Ions* (Oxford University Press, Oxford, 2012).

[40] S. Sugano, Y. Tanabe, and H. Kamimura, *Multiplets of Transition-Metal Ions in Crystals* (Academic Press, New York, 1970).

[41] V. V. Eremenko and V. P. Novikov, Davydov splitting of the exciton line in antiferromagnetic $RbMnF_3$, Zh. Eksp. Teor. Fiz. Pis. Red. **11**, 478 (1970).

[42] V. V. Eremenko, Y. G. Litvinenko, N. K. Kharchenko, and V. M. Naumenko, *Magneto-Optics and Spectroscopy of Antiferromagnets* (Springer, New York, 1992).

[43] G. F. Imbusch, Luminescence from solids with high concentrations of transition metal ions, in *Luminescence of Inorganic Solids*, edited by B. D. Bartolo, V. Godberg, and D. Pacheco (Springer, Boston, 1978), pp. 155–180.

[44] M. Boehm, S. Martynov, B. Roessli, G. Petrakovskii, and J. Kulda, Spin-wave spectrum of copper metaborate in the commensurate phase 10 K $< T <$ 21 K, J. Magn. Magn. Mater. **250**, 313 (2002).

[45] P. W. Anderson, New approach to the theory of superexchange interactions, Phys. Rev. **115**, 2 (1959).